

CHEMISTRY

A European Journal

A Journal of



Accepted Article

Title: Enhancing Photocatalytic Hydrogen Generation: The Impact of the Peripheral Ligands in Ru/Pd and Ru/Pt complexes

Authors: Nivedita Das, Gurmeet Singh Bindra, Avishek Paul, Johannes G. Vos, Martin Schulz, and Mary T. Pryce

This manuscript has been accepted after peer review and appears as an Accepted Article online prior to editing, proofing, and formal publication of the final Version of Record (VoR). This work is currently citable by using the Digital Object Identifier (DOI) given below. The VoR will be published online in Early View as soon as possible and may be different to this Accepted Article as a result of editing. Readers should obtain the VoR from the journal website shown below when it is published to ensure accuracy of information. The authors are responsible for the content of this Accepted Article.

To be cited as: *Chem. Eur. J.* 10.1002/chem.201605980

Link to VoR: <http://dx.doi.org/10.1002/chem.201605980>

Supported by
ACES

WILEY-VCH

Enhancing Photocatalytic Hydrogen Generation: The Impact of the Peripheral Ligands in Ru/Pd and Ru/Pt complexes

Nivedita Das^[a], Gurmeet Singh Bindra^{[a]#}, Avishek Paul^[a], Johannes G. Vos^[a], Martin Schulz^{*[b]} and
5 Mary T. Pryce^{*[a]}

^[a] SRC for Solar Energy Conversion, School of Chemical Sciences, Dublin City University, Dublin 9, Ireland

^[b] Friedrich Schiller University Jena, Institute of Physical Chemistry, Helmholtzweg 4, 07743 Jena, Leibniz Institut für Photonic Technology (IPHT), Albert-Einstein-Straße 9, 07745 Jena, Germany.

[#] Current address: Exigence Technologies Inc., 200-135 Innovation Drive, Winnipeg, Manitoba Canada R3T 6A8

10

Abstract

The synthesis, photophysical properties and photocatalytic efficiency of a range of new
supramolecular assemblies of the type $[\text{Ru}(\text{dceb})_2(\mu\text{-bisbpy})\text{MCl}_2](\text{PF}_6)_2$ and $[\text{Ru}(\text{bpy})_2(\mu\text{-bisbpy})\text{MCl}_2](\text{PF}_6)_2$ (where M = Pd or Pt, dceb = diethyl 2,2'-bipyridine-4,4'-dicarboxylate, bpy =
15 bipyridine and bisbpy = 2,2':5',5'':2'',2'''-quaterpyridine) are reported. Photocatalytic studies on
hydrogen generation were found to be dependent on the nature of the peripheral ligand, on the
catalytic centre and on the quantity of water present in the photocatalytic mixtures. The best catalytic
conditions were obtained with dceb as the peripheral ligand, with turnover numbers up to 513 after
hours. The experimental data together with DFT calculations on both the bpy and dceb based
20 compounds indicate that the peripheral dceb ligands participate in the photocatalytic process.

Introduction

The observation that weather patterns are now becoming more and more erratic together with the
that CO_2 levels in the atmosphere have surpassed the 400 ppm mark requires the development
25 novel environmental friendly energy resources to counteract climate change. Hydrogen as an energy
source is an attractive option, since it is carbon neutral and its application as a fuel in various energy
sectors including transport is widely promoted. However, at present the vast percentage of hydrogen
is obtained from fossil fuels, using methods that produce large amounts of CO_2 . An attractive
greener approach is the direct generation of hydrogen from water using intramolecular photocatalytic
30 assemblies capable of absorbing solar light.

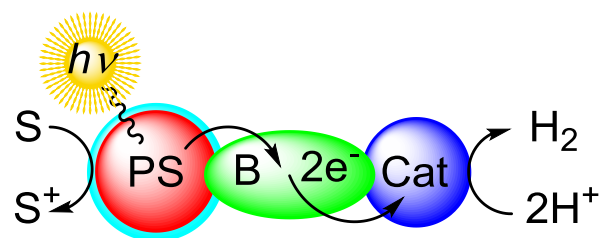


Figure 1. Intramolecular photocatalytic assembly. S = sacrificial reductant, PS = photosensitiser, Cat = catalytic centre and B = bridging ligand.

Therefore, molecular photocatalysts involving a photosensitiser and a catalytic centre have been studied using both, *inter*-molecular or *intra*-molecular pathways.¹ In the intramolecular approach photosensitiser is connected to the hydrogen generating catalytic centre via a bridging ligand shown in Figure 1.^{2,3,4} Following excitation of the sensitiser two electrons are transferred via bridging ligand to the catalytic centre most likely in a two-step process leading to the generation of hydrogen. One problem with the homogeneous approach is that sacrificial agents are required (Figure 1), that can lead to the decomposition of the photocatalytic assemblies.^{5,6} The use of sacrificial agents can be circumvented by the immobilisation of photocatalytic assemblies onto p-NiO electrode surfaces via the attachment by carboxylate based linkers.⁷

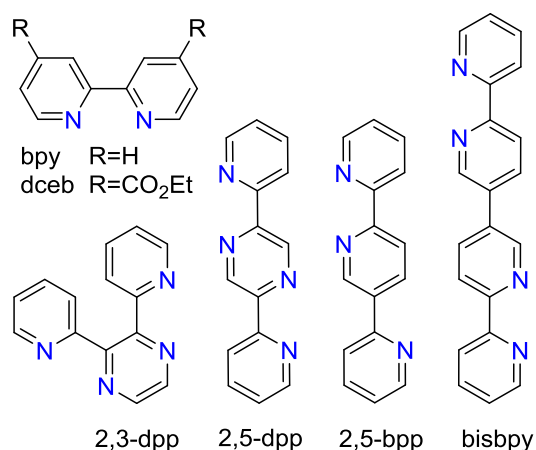


Figure 2. Bridging ligands discussed in the text; 2,2'-bipyridine (bpy), 4,4'-diethylcarboxylate-bipyridine (dceb), 2,5-di(pyridin-2-yl)pyrazine (2,5-dpp)^{4a}, 2,2':5',2''-terpyridine, (2,5-bpp)^{2b}, 2,3-di(pyridin-2-yl)pyrazine (2,3-dpp)^{3b}, 2,2':5',3'':6'',2'''-quaterpyridine (bisbpy) this work.

In a series of studies, we have investigated the introduction of carboxylate groupings at the peripheral ligands [Ru(bpy)₂]-based photosensitisers on the photocatalytic hydrogen generating capacity of molecular assemblies.³ The results obtained show that the peripheral ligands are actively involved in

the catalytic activity-determining early time excited state processes and dramatically change the electron flows in the photocatalysts.⁸ In these studies, the bridging ligands, 2,5-dpp, 2,3-dpp and 2,5-bpp (Figure 2) were used and upon the introduction of carboxylate moieties onto the peripheral ligands the TON values increased from 0 to 400 (18h) (PdCl₂ catalyst)^{3a}, 0 to 44 (18h)^{3b} (PtCl₂ catalyst) and 80 to 650 (6h)⁸ (Pt₂ catalyst) respectively. What these ligands (2,5-dpp, 2,3-bpp and 2,5-bpp) have in common is that the photosensitiser and the catalytic centre are both coordinated to the central ring. It could be argued that this may lead to a strong interaction between the two centres and that this may instigate a fast back reaction thereby limiting the photocatalytic process.

In this contribution we report our results on hydrogen evolving intramolecular assemblies based on ruthenium as the photosensitiser, together with Pd or Pt as the catalytic centres. The peripheral ligands are either unsubstituted or modified with the electron-withdrawing 4-carboxyethyl substituent as indicated in Figure 3. 2,2':5',5'':2'',2'''-quarterpyridine (bisbpy) is introduced as the bridging ligand. This compound was chosen for two reasons, firstly electrochemical measurements have shown for [Ru(bpy)₂(μ-bisbpy)Ru(bpy)₂]⁴⁺, (**Ru(bisbpy)Ru**) the bisbpy ligand is first reduced and, therefore its MLCT levels are expected to be at lower energy than those of the peripheral bpy ligands. Secondly, the bisbpy ligand conceptually consists of two bipyridine subunits connected by a free rotating single bond. Coordination of metal ions to these bipyridine subunits does not force the bisbpy ligand into a planar geometry, which is in contrast to the previously investigated bridging ligands dpp, 2,3-dpp and 2,5-bpp. Consequently, the free rotation of the bipyridine subunits may either allow for electron delocalisation over both bipyridine subunits of the bridge or it may be localised on a single bipyridine moiety. In the latter case the formation of localised bipyridine Pd- or Pt-hybrid bonding orbitals would be possible, potentially allowing for reduced electron back-transfer from the Pd- or Pt-hybrid orbital to the Ru-centre and hence improved hydrogen evolution.

The results presented in this contribution demonstrate that with dceb peripheral ligands higher TON values of up to 500 for hydrogen generation are obtained compared with those obtained with unsubstituted peripheral ligands. DFT studies on the Ru/Pd compounds suggest that the increased catalytic efficiency of the dceb type compounds may be related to a ³MLCT state where the singly occupied orbitals are localised on a bipyridine-Pd moiety located on the bridge and the dceb ligand. ¹H NMR spectroscopy indicates that upon mixing of compound **1b** with the catalytic centre [Pd(CH₃CN)₂Cl₂] *in situ*, in a 1:1 ratio results in the formation of a dinuclear complex. TON values obtained from this mixture are almost identical to those obtained from the isolated supramolecular assembly **2b**, illustrating that “*inter-molecular*” photocatalytic experiments may in fact lead to “*intra-molecular*” photocatalytic assemblies.

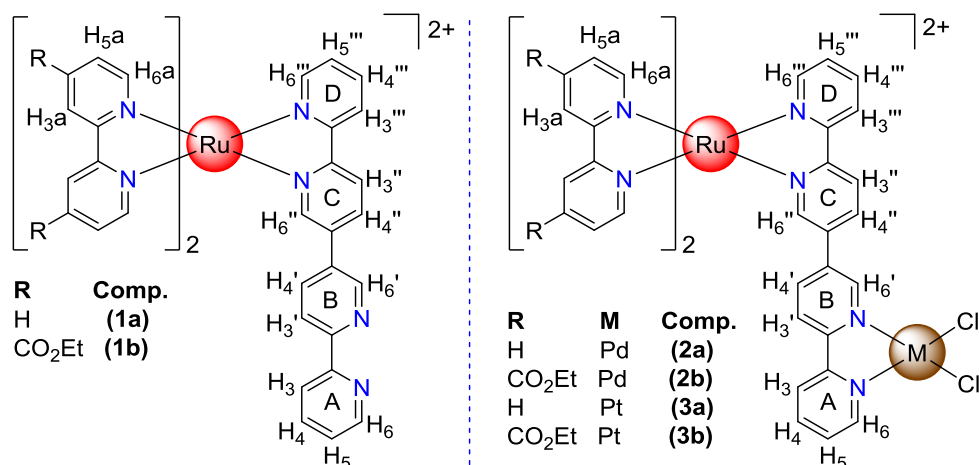


Figure 3: Molecular structures $[\text{Ru}(\text{bpy})_2(\text{bisbpy})](\text{PF}_6)_2$ (**1a**), $[\text{Ru}(\text{dceb})_2(\text{bisbpy})](\text{PF}_6)_2$ (**1b**), $[\text{Ru}(\text{bpy})_2(\mu\text{-bisbpy})\text{PdCl}_2](\text{PF}_6)_2$ (**2a**), $[\text{Ru}(\text{dceb})_2(\mu\text{-bisbpy})\text{PdCl}_2](\text{PF}_6)_2$ (**2b**), $[\text{Ru}(\text{bpy})_2(\mu\text{-bisbpy})\text{PtCl}_2](\text{PF}_6)_2$ (**3a**) and $[\text{Ru}(\text{dceb})_2(\mu\text{-bisbpy})\text{PtCl}_2](\text{PF}_6)_2$ (**3b**)

Results and Discussion

Synthesis and ^1H NMR characterisation

Recently we reported a multi-step synthesis to obtain Ru and Os based bimetallic complexes based on the bisbpy ligand. The synthesis was based on a Ni(0) catalysed cross-coupling reaction of brominated Ru and Os polypyridine precursors.^{9,10} In the present contribution this ligand is prepared in two steps using a Negishi coupling protocol. In the first step 2,5-dibromopyridine is coupled with pyridylzinc bromide yielding 5-bromo-2,2'-bipyridine followed by a Ni(0) catalysed homo-coupling of the 5-bromo species producing bisbpy with an overall yield of 60%. The presence of excess triphosphine requires careful purification (see Experimental Part). The mononuclear ruthenium complexes $[\text{Ru}(\text{bpy})_2(\text{bisbpy})]^{2+}$, (**1a**) $[\text{Ru}(\text{dceb})_2(\text{bisbpy})]^{2+}$, (**1b**) and the deuterated analogue $[\text{Ru}(\text{bpy})_2(\text{bisbpy})]^{2+}$ (**1c**) were obtained using standard procedures.³ To avoid the formation of bimetallic compounds a diluted solution containing the metal centre was added slowly to a 1.5-fold excess of bridging ligand. All compounds were fully characterised by spectroscopic methods and their purity was furthermore confirmed by elemental analysis (see Experimental Section and ESI). Some typical ^1H NMR spectra are shown in Figure 4 outlining the usefulness of partially deuterated complexes in the assignment of complicated ^1H NMR spectra. Assignments and additional spectra are shown in the experimental section and ESI respectively.

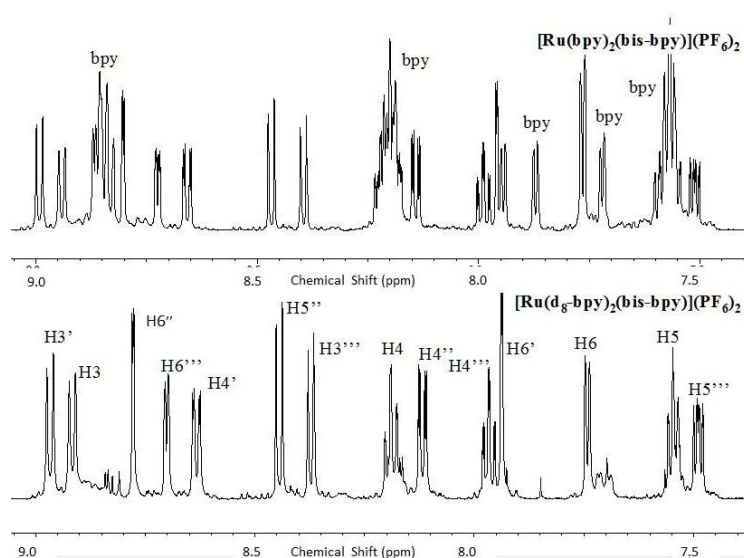


Figure 4. ^1H NMR ($\text{dms}\text{-d}_6$, 400 MHz) of (top) $[\text{Ru}(\text{bpy})_2(\text{bisbpy})](\text{PF}_6)_2$, (bottom) $[\text{Ru}(\text{d}_8\text{-bpy})_2(\text{bisbpy})](\text{PF}_6)_2$

5

Photophysical characterisation

The $^1\text{MLCT}$ transitions of **1a** closely resemble those of $[\text{Ru}(\text{bpy})_3]^{2+}$, however, a red-shifted should be evident indicating the involvement of bisbpy, which is in agreement with similar absorption features previously observed for $[\text{Ru}(\text{bpy})_2(\mu\text{-bisbpy})\text{Ru}(\text{bpy})_2]^{4+}$, (**Ru(bisbpy)Ru**) (see Table 1).⁹ Substitution of bpy to form dceb leads to a 0.31 eV redshift of the dceb-based $\pi\text{-}\pi^*$ -transition at 307 nm. The low energy $^1\text{MLCT}$ -transition is similarly red-shifted by about 0.16 eV. The introduction of palladium (**2**) or platinum (**3a-b**) results in relatively small changes in the spectral features (ESI, Figure S4-S6). Emission maxima for the bimetallic compounds do not vary greatly when compared with the precursor compounds (Table 1, ESI, Figure S4-S6). Compound **1a** emits at 633 nm, while the emission maximum of the RuPd analogues **2a** and **3a** is shifted to lower energy by between 0.07-0.09 eV. Similar emission profiles were obtained for compounds **1b**, **2b** and **3b**.

The observed emission quantum yields of all investigated compounds are low and in the range between about 2-10%. However, for the dinuclear compounds **2b**, **3a** and **3b** reduced lifetimes were observed which correlate with decreased emission quantum yields. Compound **2a** is an exception, showing a decreased lifetime but without significant change of the quantum yield. This indicates an increased radiative rate, probably due to increased spin-orbit coupling and was previously observed for $[\text{Ru}(\text{bpy})_2(\mu\text{-2,5-bpp})\text{PdClSolvent}]^{2+}$.^{3a,12} Furthermore, as shown in Table 1, mono-exponential decays were observed for **1a** and **1b**, and for the Pd based photocatalysts **2a** and **2b** dual exponential decays are observed (see ESI, Figure S8-S10). A dual emission decay is unusual, but we have previously observed this for another Ru-Pd type photocatalyst involving the 2,5-bpp bridging ligand

5

(cf. Fig. 2).¹² For this compound two lifetimes of 400 (37%) and 88 (63%) ns were observed, which are most likely associated with emission from the ³MLCT based on bpy peripheral and the bridging ligand respectively. Further experiments are needed study the reasons for the dual exponential decay observed for compounds **2a** and **2b**.

5

Table 1 Photophysical properties of the compounds **1a-b**, **2a-b**, **3a-b** and related compounds.

Compounds	$\lambda_{\text{abs, max}}$ [nm]	$\lambda_{\text{em, max}}^{\text{a}}$ [nm]	τ^{b} (ns)	Φ^{c}
	(ϵ in $10^4 \text{ M}^{-1} \text{ cm}^{-1}$)	293 K	293 K	293K
1a	448 (1.16)	633	755	0.040
1b	475 (1.13)	647	825	0.101
2a	447 (1.02)	655	17 (37%) 218 (63%)	0.044
2b	475(1.76)	647	42 (60 %) 325 (40%)	0.033
3a	447 (1.15)	664	331	0.017
3b	475 (1.63)	644	534	0.054
Ru(μ -bisbpy)Ru	440 (2.53)	663	215*	N/A ⁹
[Ru(bpy) ₃] ²⁺	450 (1.30)	605	860	0.068 ¹¹
[Ru(dceb) ₂ (μ -2,5-bpp)PtI Solvent] ²⁺	483 (1.65)	662	624	-----8
[Ru(bpy) ₂ (μ -2,3-dpp)PtI ₂] ²⁺	516 (4.32)	778 (vw)	-	-----3b
[Ru(dceb) ₂ (μ -2,3-dpp)PtI ₂] ²⁺	485(4.25)	-	-	-----3b
[Ru(bpy) ₂ (μ -2,5-dpp)PdCl ₂] ²⁺	539(4.00)	807	<0.5	-----3a
[Ru(dceb) ₂ (μ -2,5- dpp)PdCl ₂] ²⁺	526(4.20)	778	<0.5	-----3a

^a Excitation at 455 nm. ^bLifetime determined by TCSPC at 293 K in deaerated acetonitrile solution ($\lambda_{\text{exc.}} = 360$). ^cQuantum Yields determined at 293 K in deaerated acetonitrile at $\lambda_{\text{exc.}} = 455$ nm, solvent, * = aerated; N/A = not available.

10

Photocatalysis

The complexes **2a-b** and **3a-b** were tested as photocatalysts for hydrogen production. Mixtures of photocatalyst and the sacrificial donor (triethylamine, TEA), were irradiated at 470 nm in acetonitrile solutions with varying water content (for further details see experimental section). Control experiments did not produce any hydrogen. Intermolecular studies were also carried out with solutions containing equimolar mixtures of the photosensitiser **2b** and a Pd catalyst. All results obtained are listed in Table 2. The data listed in Table 2 show that the TONs obtained are dependent on both the nature of the reaction mixture, *i.e.* the amount of water present and the moieties present on the peripheral ligands

6

of the photocatalysts. They indicate that the best TON values, are obtained in the presence of 5% water. Therefore, the discussion is mainly focused on these results. The results obtained indicate that the catalytic process is more efficient for the compounds, **2b** and **3b**, and that the Pd catalysts are more effective than their Pt analogues, as has also been found by others.¹⁴ Similarly to the enhancement in the TONs observed for complex **2b** (when compared to **2a**), the TON value acquired for the platinum analogue **3b** is also substantially greater than that of **3a**, thereby further indicating the strongly enhanced photocatalytic efficiency in the presence of dceb peripheral ligands. We note that in the presence of 0% and 15% of water the Pt compound **3a** (bpy ligands) shows a higher TON value than the associated Pt compound **3b** which contains carboxy based ligands. In addition **3a** is more efficient than the Pd analogue **2a**. The Pd compound **2b** remains the better photocatalyst in solutions containing 15% water. These observations are at present not understood and further studies are needed to explain these behaviour.

Table 2 Turnover numbers (TONs) for photocatalytic hydrogen generation.

Compounds	TON ^a as function of water content (v/v)			
	0%	5%	10%	15%
2a	0	5	16	13
2b	23	513	360	198
3a	29	75	92	85
3b	13	258	286	45
1b + [Pd(CH ₃ CN) ₂ Cl ₂] ^b	n.d.	489	321	n.d.
1a	0	0	0	0
1b	0	0	0	0
[Pd(CH ₃ CN) ₂ Cl ₂]	0	0	0	0
[Pt(dmsO) ₂ Cl ₂]	0	0	0	0
TEA	0	0	0	0
[Ru(bpy) ₂ (μ-2,5-bpp)PtI Solvent] ²⁺			100	--- ⁸
[Ru(dceb) ₂ (μ-2,5-bpp)PtI Solvent] ²⁺			720	--- ⁸
[Ru(bpy) ₂ (μ-2,3-dpp)PtI ₂] ²⁺			0	--- ^{3b}
[Ru(dceb) ₂ (μ-2,3-dpp)PtI ₂] ²⁺			44	--- ^{3b}
[Ru(bpy) ₂ (μ-2,5-dpp)PdCl ₂] ²⁺		0		--- ^{3a}
[Ru(dceb) ₂ (μ-2,5-dpp)PdCl ₂] ²⁺		400		--- ^{3a}

^a Determined by GC following irradiation (irradiation wavelength = 470 nm) for 18 h. The TON values are averages of three samples and could be determined with a standard deviation of 12% or better.^b

The reaction mixture contains an equimolar mix of the mononuclear complex and Pd catalysts (4.08×10^{-5} M), and triethylamine 2.15 M and varies percentages of water (0-15%). n.d = not determined.

The TONs obtained for the complexes **2b** and **3b** containing dceb as peripheral ligands are 513 and 258 respectively. These TONs are considerably higher than obtained for the bpy analogues **2a** and **3a** which yielded values of 5 and 75 respectively. A similar dependence of the catalytic performance on the peripheral ligand was recently reported for the $[\text{Ru}(\text{dceb})_2(2,5\text{-dpp})\text{PdCl}_2]^{2+}$ complex with a value of 400 (18 h) with the bpy analogue, $[\text{Ru}(\text{bpy})_2(2,5\text{-dpp})\text{PdCl}_2]^{2+}$ not producing any detectable amounts of hydrogen (for bridging ligand see Fig. 2).^{3a}

Another important observation is that the photocatalytic efficiency observed for the supramolecular assembly **2b** is very similar to that observed for the mixture of **1b** and $[\text{Pd}(\text{CH}_3\text{CN})_2\text{Cl}_2]$. To further investigate this observation the time dependence of both processes was investigated under identical photocatalytic conditions. The results obtained are shown in Figure 5. This Figure shows that both systems reach a plateau after ~ 8 h with a TON value of about 480 but are still producing hydrogen after 18 h of irradiation reaching a TON of about 510. For **2b** no lag phase is observed, but for mixture of **1b** and $[\text{Pd}(\text{CH}_3\text{CN})_2\text{Cl}_2]$ a small delay at the start of the photocatalytic process is observed. However, the turnover frequencies obtained after 2 hours (TOF) are similar in both instances with a value of about 60 h^{-1} for **2b** while for the mixture of **1b** and $[\text{Pd}(\text{CH}_3\text{CN})_2\text{Cl}_2]$ a value of about 50 h^{-1} is obtained and at longer times the TOF values remain comparable. The similarity in the quantities of hydrogen produced and of the hydrogen generation profile with time suggests the *in situ* formation of a dinuclear species. This issue is further investigated with ^1H NMR and the results obtained from these studies are shown in the ESI. It is important to note that the concentrations of the reactants used in the NMR studies are more than an order of magnitude higher than those in the photocatalysis studies. As a result in the NMR studies containing a mixture of **1b** and $[\text{Pd}(\text{CH}_3\text{CN})_2\text{Cl}_2]$ an intramolecular species is formed after ~5 min, while in the photocatalysis experiments the formation of the intramolecular compound is slower.

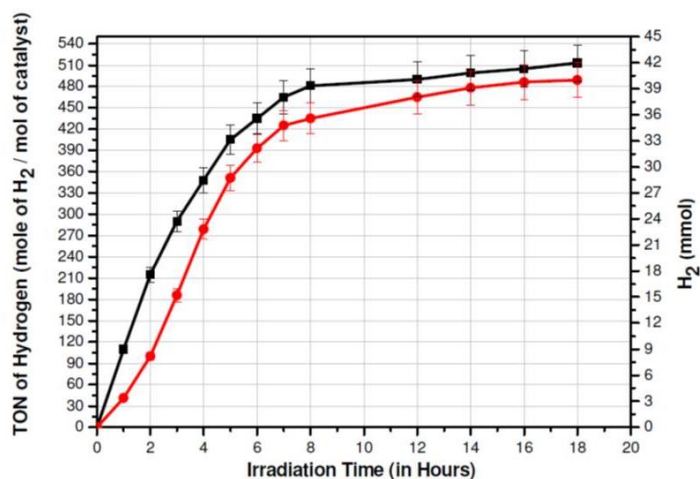


Figure 5. Time-dependence of the TON achieved for H₂ evolution for **2b** (black line) and **1** [Pd(CH₃CN)₂Cl₂] (red line).

5 Computational results

Recently we have studied photocatalysts containing the 2,5-bpp ligand.^{12,15} In this contribution we have extended our studies to include the bisbpy bridging ligand. As outlined above this ligand is different from the earlier used bpp and dpp type ligands, since the photosensitizer and the catalyst center are now bound to different parts of the bridging ligand through coordination bonds rather than through the same ring by cyclometallation. In this section DFT studies are used to further investigate the electronic properties of the compounds reported here. For details on the methods and parameters used see the experimental part. To reduce the computational costs the decyl ethyl ester groups were replaced by methyl esters therefore the compounds **2a** and **2b** are now labelled as **2a'** and **2b'** (Figure 3). In these studies the location of the molecular orbitals associated with the singlet ground state (SGS), the lowest energy triplet state (³MLCT) and the singly-reduced doublet (SRDS) states were investigated. The latter state is essentially a ground state with an added electron and could be obtained by reductive quenching after photoexcitation. The location of the frontier orbitals was evaluated by a population analysis of the optimised dinuclear Ru-Pd complexes (see ESI, Tables S7). In the singlet ground states of both **2a'** and **2b'** the three highest energy occupied orbitals are ruthenium based orbitals as expected (HOMO, H-1, H-2). The LUMO for **2a'** is bridge-based, however, for **2b'** the LUMO is a mixed orbital which is located on both the peripheral MeOOC-bpy ligands (63%) and the bridging ligand (35%). The orbitals associated with the singly reduced species SRDS of **2a'** (doublet state, overall charge is +1) are based on the bridging ligand (*cf.* α-MO 197 in Table S4, ESI), while this orbital is found on the MeOOC-bpy peripheral ligand for **2b'** (*cf.* α-MO 257 in Table S7, ESI). The lower lying doubly occupied orbitals are Ru-based as expected. Population analysis of the lowest energy triplet states in **2a'** and **2b'** reveals that for **2a'** both singly occupied

orbitals are bridge-based (*cf.* Fig.6a,b and α -MOs 197-196 in Table S3, ESI). However, for **2b'** the high energy singly occupied orbital is based on the peripheral MeOOC-bpy ligand while the low energy singly occupied orbital is a hybrid bridging ligand-PdCl₂ orbital (*cf.* Fig.6c and Fig. 6d respectively see also and α -MO 257-256 in Table S6, ESI). The differences in the electronic situation are also reflected by the torsion angle between the 2,2'-bipyridine moieties that make up the bisbpy bridging ligand. For **2a'** the torsion angle of 17.1° is considerably smaller than for **2b'** (35.5°) owing to the delocalisation of the unpaired electrons on the bridging ligand in the former case and their localisation on the peripheral ligand and on a hybrid bridging ligand/PdCl₂ orbital in the latter.

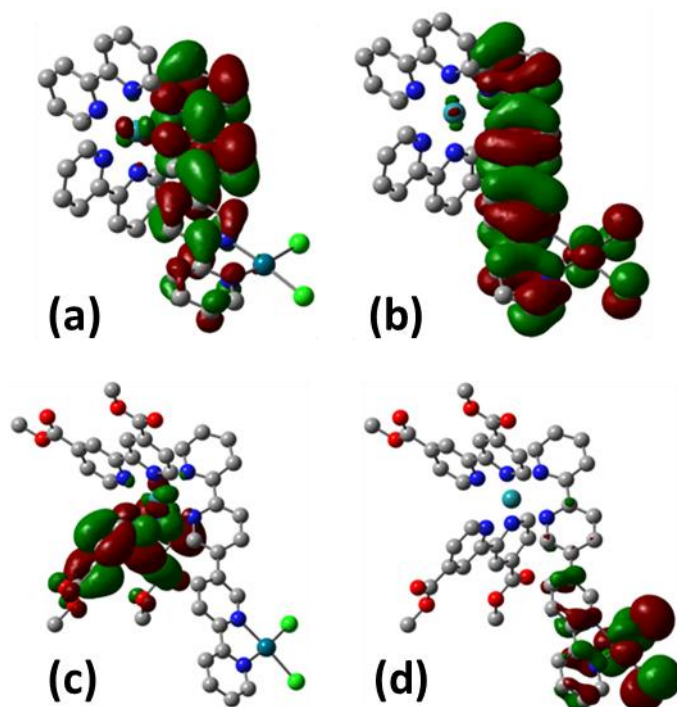


Figure 6: DFT representation of the two singly occupied orbitals of the lowest energy triplet state **2a'** (a, b) and **2b'** (c, d)

The complexes reported in this contribution are part of a series of compounds published by our group where we have investigated a range of Ru-Pd and Ru-Pt dyads with various bridging (see Figure 15 and peripheral ligands using the same experimental conditions.^{3,8,12,15} As observed for the compounds investigated in this contribution, their catalytic activity as hydrogen evolving catalysts was found to be dependent on changes on the bridging or on the peripheral ligands. Of interest in this respect is a recent ultrafast transient absorption and resonance-Raman investigation on the hydrogen evolving $[\text{Ru}(\text{bpy})_2(2,5\text{-bpp})\text{-PdCl}(\text{acetonitrile})]^{2+}$ (for bridging ligand see Fig. 2).¹² In this recent publication we demonstrated that excitation of $[\text{Ru}(\text{bpy})_2(2,5\text{-bpp})\text{-PdCl}(\text{acetonitrile})]^{2+}$ at 470 nm resulted in

population of $^1\text{MLCT}$ states on the peripheral bpy- and the 2,5-bpp bridging ligand, followed by intersystem crossing into the corresponding hot $^3\text{MLCT}$ states.¹² Furthermore, it was shown that electron density localised on the bpy ligand cannot flow to the bridging 2,5-bpp ligand, this will limit electron transfer to the bridging ligand and will reduce hydrogen generation. This is confirmed by the
5 detection of two emission channels indicating that electron density remains on the peripheral bpy ligand. Efficient interligand electron transfer is important for efficient hydrogen evolution but this is not observed for standard, unsubstituted, bpy ligands. However, it was suggested that this can be achieved by the introduction of functionalised peripheral ligands. Our later studies involving peripheral ligands modified with ester groupings have confirmed this.

10

A second aspect raised by the investigation in ref. 12 is the localisation of the electron density : the interligand electron transfer process and subsequent transfer to the catalytically active m centre. This ligand-to-metal electron transfer process competes with the decay of the $^3\text{MLCT}$ stat the bridging 2,5-bpp ligand to the ground state, thus limiting hydrogen evolution. It was argued
15 the population of a hybrid orbital formed between the bridging 2,5-bpp ligand and the Pd centre | be beneficial for intermediate electron storage and subsequent proton reduction.

The DFT results obtained in this contribution provide direct evidence for such an orbital. The obser superior catalytic activity of the dceb complex **2b**, with respect to the bpy complex **2a**, is in line the DFT results for **2b'** showing localised orbitals based on the peripheral dceb ligand as well as
20 the PdCl_2 binding part of the bisbpy ligand. In contrast, the delocalised singly occupied orbitals fc for the $^3\text{MLCT}$ state of **2a'** are most likely disadvantageous for the catalytic process, since the str coupling may also enhance electron recombination to the singlet ground state. The bisbpy brid ligand is able to adopt both configurations which allows strong coupling via delocalised elec density as well as localised electron density by virtue of a free rotating single bond, which connect
25 bipyridine subunits. Interestingly, it is the peripheral ligand that causes the formation of either on these configurations. Despite the possibility of free rotating subunits in the bisbpy bridge, the im on the hydrogen generation performance of complexes with different bridging ligands but with dceb peripheral ligands is less dramatic than with the same bridge but different peripheral ligands Table 2). However, great care has to be taken in this discussion since the catalytic performanc
30 certainly influenced by a range of (partly unknown) parameters. Moreover, no information is available on the nature of the catalytically active species. Such species are of great importance but are experimentally difficult to detect.

Conclusions

35 In this contribution we report the synthesis and characterisation of novel *intra*-molecular Ru/Pd and

Ru/Pt complexes tethered to the bisbpy bridging ligand. This work is part of a series of systematic studies aimed at investigating the influence of bridging ligands, peripheral ligands and the nature of catalytic centres may have on light driven hydrogen generation.^{3,4,8,12,15} The most striking observation in the present investigations is that much increased TON numbers are obtained when the peripheral dceb ligands are introduced irrespective of the nature of the bridging ligand or catalytic centre. However, emission data indicate that emission decays are different for Pd and Pt containing complexes and hence the electron flows in those complexes. In an earlier study¹⁵ transient absorption measurements indicated the dceb ligands most likely act as electron storage ligands, contrary to what is expected in the traditional assumption that the electron density is stored on the bridging ligand.⁸ The present contribution supports this perception, based on the obtained experimental and DFT calculations. The latter indicate the presence of an electronic configuration with one singly occupied Pd-br hybrid orbital and one on the dceb peripheral ligands. The data presented emphasise, that even relatively small structural changes can have a large impact on the catalytic efficiency. Finally pointed out in the introduction, for the design of a sustainable technology, immobilisation of photocatalysts on electrode surfaces is necessary. This contribution shows that the introduction of anchoring carboxylate moieties onto the peripheral ligands can have a dramatic influence on hydrogen generation efficiency and underlines the need for well-balanced energy levels between three components of the *intra*-molecular photocatalyst, *i.e.* photosensitiser, bridging ligand and catalytic centre.

Experimental Section

The compounds 2,2'-bipyridine (bpy), $\text{RuCl}_3 \cdot \text{H}_2\text{O}$ and $[\text{Pd}(\text{CH}_3\text{CN})_2\text{Cl}_2]$ are from Aldrich. The synthesis of $[\text{Ru}(\text{bpy})_2\text{Cl}_2] \cdot 2 \text{H}_2\text{O}$ ¹⁶, $[\text{Ru}(\text{d}_8\text{-bpy})_2\text{Cl}_2] \cdot 2\text{H}_2\text{O}$ ¹⁷, $[\text{Ru}(\text{dceb})_2\text{Cl}_2] \cdot 2\text{H}_2\text{O}$ ⁸ and $[\text{Pt}(\text{dmsO})_2]$ are reported elsewhere.

2,2':5',5'':2'',2'''-quaterpyridine (bisbpy)

Step-1: Under nitrogen atmosphere $\text{Pd}(\text{PPh}_3)_4$ (0.3 g, 0.26 mmol) and 2,5-dibromobipyridine (2.8.44 mmol) were added to a dried two neck round bottom flask and cooled to 0°C. Upon addition of pyridylzinc bromide in THF (19.4 cm³, 8.44 mmol) the reaction mixture turned brown in colour and was then stirred over night at room temperature under inert atmosphere while a white precipitate formed. Subsequently the reaction mixture was poured in to 200 cm³ of a saturated aqueous solution of equimolar EDTA and Na_2CO_3 and stirred until the white solid turned completely yellow. The aqueous suspension extracted with dichloromethane (3 × 50 cm³), the combined organic layers were dried over sodium sulphate and the solvent was evaporated by vacuum. The obtained crude product was purified on an activated neutral alumina (150 mesh size) column using hexane/ethylacetate

(9.5:0.5 v/v), monitored by TLC (second spot, $R_f = 0.2$) and yielded 5-bromo-2,2'-bipyridine (81 %).

Step-2: $[\text{Ni}(\text{PPh}_3)_2\text{Cl}_2]$ (0.557 g, 0.85 mmol) was added in to 10 cm³ of anhydrous DMF and stirred for few minutes at room temperature under nitrogen atmosphere, until the mixture turned blue. After addition of zinc powder (0.056 g, 0.85 mmol) the mixture was stirred at room temperature under nitrogen atmosphere for 45 min while the colour turned green and ultimately deep brown. Subsequently, 5-bromo-2,2'-bipyridine (0.200 g, 0.85 mmol) was added and the reaction mixture was stirred at room temperature for 10 hours and was then poured into 150 cm³ of 3 molar aqueous NH_4OH solution while a greyish product precipitated. The precipitate was extracted with ethyl acetate (3 × 50 cm³) and the combined organic phases were dried over MgSO_4 . Removal of the solvent in vacuo yielded the crude product which was purified by column chromatography (neutral alumina, hexane/ethyl acetate (9:1 v/v), TLC: $R_f = 0.1$) to obtain 2,2':5',5'':2'',2'''-quaterpyridine in 78 % yield. Anal. Calcd. for $\text{C}_{20}\text{H}_{14}\text{N}_4 \cdot 0.2 \text{H}_2\text{O}$ (313.95): C, 76.51; H 4.62; N, 17.85%. Found: C, 76.84; H, 4.63; N, 17.24%. ¹H-NMR (dms $\text{O}-d_6$, 400 MHz): $\delta = 7.50$ (dd, 2H, J = 7.4 Hz, J = 2.5 Hz, J = 1.1 Hz, H-5'''), 8.00 (dd, 2H, J = 7.8 Hz, J = 2.0, H-4, H-4'''), 8.43 (dd, 2H, J = 8.3 Hz, J = 2.5 Hz, H-4', H-4'''), 8.46 (dd, 2H, J = 7.8 Hz, J = 1.0 Hz, H-3, H-3'''), 8.54 (dd, 2H, J = 8.0 Hz, J = 1.0 Hz, H-3', H-3'''), 9.18 (d, 2H, J = 2.5 Hz, H-6', H-6'').

$[\text{Ru}(\text{bpy})_2(\text{bisbpy})](\text{PF}_6)_2 \cdot 2 \text{H}_2\text{O}$ (**1a**)

$[\text{Ru}(\text{bpy})_2\text{Cl}_2] \cdot 2 \text{H}_2\text{O}$ (0.34 g, 0.65 mmol) dissolved in 5 cm³ of ethanol was added drop-wise solution of bisbpy (0.26 g, 0.85 mmol) in 10 cm³ of ethanol/water (3:1 v/v). The reaction mixture refluxed for 8 hours and then allowed to cool to room temperature and the solvent was evaporated under vacuum. To the residue, 2 cm³ of deionized water was added in order to dissolve the product and excess bisbpy was filtered off. Subsequently, the product was precipitated by addition of KI to the filtered solution. The precipitate was washed twice with a total of 5 cm³ of water and 10 cm³ diethylether. Recrystallization from acetone/water (3:1 v/v) afforded a red solid. Yield: 0.588 g (0.65 mmol, 86%). Anal. Calcd. for $\text{C}_{40}\text{H}_{30}\text{F}_{12}\text{N}_8\text{P}_2\text{Ru} \cdot 2 \text{H}_2\text{O}$ (1049.75): C, 45.77; H, 3.26; N, 10.6%. Found: C, 46.15; H, 2.86; N, 10.29%. ¹H-NMR (Acetonitrile- d_3 , 400 MHz): $\delta = 8.72$ -8.68 (m, 2H, H-6'), 8.65 (d, 1H, J = 8.0 Hz, H-3''), 8.58 (d, 1H, J = 7.8 Hz, H-3'''), 8.62-8.50 (m, 4H, bpy (H-4, H-4')), 8.45- 8.39 (m, 2H, H-3', H-4''), 8.15-8.05 (m, 5H, bpy (H-4a), H-4'''), 7.97-7.89 (m, 4H, H-3, H-4, H-4'), 7.83 (d, 1H, J = 4.8 Hz, bpy (H-6a)), 7.79-7.72 (m, 4H, bpy (H-6a), H-6'''), 7.47-7.39 (m, 6H, bpy (H-5a), H-5, H-5''').

$[\text{Ru}(\text{dceb})_2(\text{bisbpy})](\text{PF}_6)_2 \cdot 2\text{CH}_3\text{COCH}_3$ (**1b**)

$[\text{Ru}(\text{dceb})_2\text{Cl}_2] \cdot 2 \text{H}_2\text{O}$ (0.52 g, 0.65 mmol) dissolved in 5 cm³ of ethanol was added drop-wise to a solution of bisbpy (0.26 g, 0.80 mmol) in 10 cm³ of ethanol/water (3:1 v/v). The reaction mixture was

refluxed for 8 hours and then allowed to cool to room temperature and the solvent was evaporated under vacuum. Subsequently, the product was precipitated by addition of KPF_6 to the filtered solution. The precipitate was washed twice with a total of 5 cm^3 of water and 10 cm^3 of diethylether. Recrystallization from acetone/water (3:1 v/v) afforded a red solid. Yield: 0.765 g (0.54 mmol, 83%).
 5 Anal. Calcd. for $\text{C}_{52}\text{H}_{46}\text{F}_{12}\text{N}_8\text{P}_2\text{Ru} \cdot 2 \text{CH}_3\text{COCH}_3$ (1418.26): C, 49.12; H, 4.12; N, 7.90%. Found: C, 49.42; H, 4.14; N, 7.84%. $^1\text{H-NMR}$ (Acetonitrile- d_3 , 400 MHz): $\delta = 9.13$ - 9.08 (m, 4H, bpy (H-3a)), 8.74-8.66 (m, 3H, H-3", H-6, H-6'), 8.61 (d, 1H, $J = 8.0$ Hz, H-3'''), 8.46 (m, 1H, H-4"), 8.42 (d, 1H, $J = 7.8$ Hz, H-3'), 8.16 (ddd, 1H, $J = 7.8$ Hz, $J = 2.0$, H-4'''), 8.12 (d, 1H, $J = 4.8$ Hz, bpy (H-6a)), 8.00-7.82 (m, 11H, bpy (H-6a, H-5a), H-3, H-4, H-4', H-6"), 7.69 (d, 1H, $J = 4.8$ Hz, H-6'''), 7.48-7.42 (m, 2H, H-5
 10 5'''), 4.52-4.43 (m, 8H, CH_2), 1.46-1.40 (m, 12H, CH_3), 2.10 (s, 12H, CH_3 , acetone).

$[\text{Ru}(\text{d}_8\text{-bpy})_2(\text{bisbpy})](\text{PF}_6)_2 \cdot \text{H}_2\text{O}$ (**1c**)

This complex was synthesised following the procedure used for complex **1a**. 86 mg (0.28 mmol) bisbpy and 100 mg (0.18 mmol) of $[\text{Ru}(\text{d}_8\text{-bpy})_2\text{Cl}_2] \cdot \text{H}_2\text{O}$ were reacted. Yield: 137 mg (0.133 mmol, 71%).
 15 $^1\text{H NMR}$ (600 MHz, $\text{dms-}d_6$) δ ppm 7.49 (dd, $J = 7.34, 4.71$, Hz, H5'''), 7.55 (dd, $J = 7.15, 4.71$, Hz, H5), 7.74 (d, $J = 5.65$ Hz, H6'''), 7.94 (s, H6''), 7.97 (d, $J = 7.72, 1.51$ Hz, H4'''), 8.12 (dd, $J = 8.28, 2.45$ Hz, H4''), 8.19 (m, H4), 8.37 (d, $J = 7.91$ Hz, H3'''), 8.44 (d, $J = 8.28$ Hz, H3''), 8.63 (dd, $J = 8.28, 2.07$ Hz, H4'), 8.70 (d, $J = 4.14$ Hz, H6), 8.78 (s, H6'), 8.92 (d, $J = 8.28$ Hz, H3), 8.97 (d, $J = 8.28$ Hz, H3'). Anal. Calcd. for $\text{C}_{40}\text{H}_{16}\text{D}_{16}\text{F}_{12}\text{N}_8\text{OP}_2\text{Ru}$: C 45.8, H 3.0, N 10.4. Found: C 46.2, H 2.7 and N 10.0
 20

$[\text{Ru}(\text{bpy})_2(\mu\text{-bisbpy})\text{PdCl}_2](\text{PF}_6)_2 \cdot 2\text{H}_2\text{O}$ (**2a**)

1a (0.100 g, 0.095 mmol) dissolved in 5 cm^3 of dichloromethane was added drop-wise to a solution of $[\text{Pd}(\text{CH}_3\text{CN})_2\text{Cl}_2]$ (0.025 g, 0.095 mmol) in 5 cm^3 of dichloromethane. The reaction mixture refluxed for 24 hours and then allowed to cool to room temperature. Subsequently, the product precipitated by addition of 5 cm^3 of diethylether, filtered and washed twice with a total of 10 cm^3 diethylether. Recrystallization from acetone/water (3:1 v/v) afforded a red solid. Yield: 0.115 g (0.095 mmol, 99%).
 25 Anal. Calcd. for $\text{C}_{40}\text{H}_{30}\text{F}_{12}\text{Cl}_2\text{N}_8\text{P}_2\text{RuPd} \cdot 2 \text{H}_2\text{O}$ (1226.5): C, 39.14; H, 2.70; N, 9.96%. Found: C, 39.29; H, 2.50; N, 8.83. $^1\text{H-NMR}$ (Acetonitrile- d_3 , 400 MHz): $\delta = 9.21$ (d, 1H, $J = 4.8$ Hz, H-6), 9.17 (d, 1H, $J = 2.5$ Hz, H-6'), 8.67 (d, 1H, $J = 8.0$ Hz, H-3''), 8.63-8.57 (m, 3H, bpy (H-3a), H-3b), 8.54-8.50 (m, 2H, bpy (H3a)), 8.43-8.37 (m, 2H, H-4', H-4''), 8.30 (d, 1H, $J = 7.8$ Hz, H-3'), 8.26-8.21 (m, 2H, H-3, H-4), 8.13-8.05 (m, 5H, bpy (H-4a), H-4'''), 8.02 (d, 1H, $J = 2.3$ Hz, H-6''), 7.89 (d, 1H, $J = 4.8$ Hz, bpy (H-6a)), 7.79-7.74 (m, 4H, bpy (H-6a), H-6'''), 7.70 (m, 1H, H-5), 7.48-7.39 (m, 5H, bpy (H-5a), H-5'').
 30

$[\text{Ru}(\text{dceb})_2(\mu\text{-bisbpy})\text{PdCl}_2](\text{PF}_6)_2 \cdot 2 \text{H}_2\text{O}$ (**2b**)

1b (0.100 g, 0.071 mmol) dissolved in 5 cm³ of dichloromethane was added drop-wise to a solution of [Pd(CH₃CN)₂Cl₂] (0.018 g, 0.071 mmol) in 5 cm³ of dichloromethane. The reaction mixture was refluxed for 24 hours and then allowed to cool to room temperature. Subsequently, the product was precipitated by addition of 5 cm³ of diethylether, filtered and washed twice with a total of 10 cm³ of diethylether and 10 cm³ of n-hexane. Recrystallization from acetone/water (3:1 v/v) afforded a red solid. Yield: 0.112 g (0.070 mmol, 98%). Anal. Calcd. for C₅₂H₄₆F₁₂O₈Cl₂N₈P₂RuPd · 2H₂O (1515.29): C, 41.21; H, 3.29; N, 7.39; Found: C, 41.12, H, 3.22, N, 6.67. ¹H-NMR (Acetonitrile-d₃, 400 MHz): δ = 9.21 (d, 1H, J = 4.8 Hz, H-6), 9.19 (d, 1H, J = 2.5 Hz, H-6'), 9.13-9.10 (m, 2H, bpy (H-3a), 9.08-9.05 (m, 2H, bpy (H-3a), 8.67 (d, 1H, J = 8.0 Hz, H-3''), 8.62 (m, 1H, J = 7.8 Hz, H-3'''), 8.47-8.43 (m, H-4', H-4''), 8.27 (d, 1H, J = 8.0 Hz, H-3'), 8.26-8.21 (m, 2H, H-3, H-4), 8.16 (ddd, 1H, J = 7.8 Hz, 2.4 Hz, H-4'''), 8.11 (d, 1H, J = 4.8 Hz, bpy (H-6a)), 8.00 (d, 1H, J = 2.3 Hz, H-6''), 7.97-7.90 (m, bpy (H-6a, H-5a)), 7.72-7.66 (m, 2H, H-5, H-6'''), 7.48 (ddd, 1H, J = 4.8 Hz, J = 1.0 Hz H-5'''), 5.41 2H, CH₂, CH₂Cl₂), 4.52-4.44 (m, 8H, CH₂, ethyl-ester), 1.46-1.41 (m, 12H, CH₃, ethyl-ester).

[Ru(bpy)₂(μ-bisbpy)PtCl₂](PF₆)₂ · 3H₂O (**3a**)

1a (0.100 g, 0.095 mmol) dissolved in 5 cm³ of dichloromethane was added drop-wise to a solution of [Pt(dmso)₂Cl₂] (0.042 g, 0.095 mmol) in 5 cm³ of dichloromethane. The reaction mixture was refluxed for 24 hours and then allowed to cool to room temperature. Subsequently, the product was precipitated by addition of 5 cm³ of diethylether, filtered and washed twice with a total of 10 cm³ of diethylether. Recrystallization from acetone/water (3:1 v/v) afforded a red solid. Yield: 0.109 g (0.095 mmol, 86%). Anal. Calcd. for C₄₀H₃₀F₁₂Cl₂N₈P₂RuPt · 3 H₂O (1334.2): C, 35.97; H, 2.60; N, 8.00; Found: C, 35.70; H, 2.35; N, 7.95. ¹H-NMR (Acetonitrile-d₃, 400 MHz): δ = 9.54 (d, 1H, J = 2.5 Hz, H-6'), 9.51 (d, 1H, J = 4.8 Hz, H-6), 8.69 (d, 1H, J = 8.0 Hz, H-3''), 8.63-8.58 (m, 3H, bpy (H-3a), H-3a'), 8.55-8.51 (m, 2H, bpy (H-3a)), 8.47-8.40 (m, 2H, H-4', H-4''), 8.30-8.23 (m, 2H, H-3', H-4), 8.16 (ddd, 1H, J = 7.8 Hz, H-3), 8.14-8.04 (m, 6H, bpy (H-4a), H-4''', H-6''), 7.92 (d, 1H, J = 4.8 Hz, bpy (H-6a)), 7.79-7.74 (m, 4H, bpy (H-6a), H-6'''), 7.70 (m, 1H, H-5), 7.48-7.39 (m, 5H, bpy (H-5a), H-5''').

[Ru(dceb)₂(μ-bisbpy)PtCl₂](PF₆)₂ (**3b**)

1b (0.100 g, 0.071 mmol) dissolved in 5 cm³ of dichloromethane was added drop-wise to a solution of [Pt(dmso)₂Cl₂] (0.030 g, 0.071 mmol) in 5 cm³ of dichloromethane. The reaction mixture was refluxed for 24 hours. Subsequently, the product was precipitated by addition of 5 cm³ of diethylether, filtered and washed twice with a total of 10 cm³ of diethylether and 10 cm³ of n-hexane. Recrystallization from acetone/water (3:1 v/v) afforded a red solid. Yield: 0.115 g (0.068 mmol, 96%). Anal. Calcd. for C₅₂H₄₆F₁₂O₈Cl₂N₈P₂RuPt (1567.95): C, 39.83; H, 2.96; N, 7.15; Found: C, 39.97, H, 3.24; N, 6.25. ¹H-NMR (Acetonitrile-d₃, 400 MHz): δ = 9.57 (d, 1H, J = 2.5 Hz, H-6'), 9.49 (d, 1H, J = 4.8 Hz, H-6), 9.13-

9.10 (m, 2H, bpy (H-3a)), 9.08-9.02 (m, 2H, bpy (H-3a)), 8.72 (d, 1H, J = 8.0 Hz, H-3"), 8.63 (m, 1H, J = 7.8 Hz, H-3"), 8.47-8.40 (m, 2H, H-4', H-4"), 8.23 (t, 1H, J = 7.8 Hz, H-4), 8.19-8.09 (m, 4H, bpy (H-6a), H-3, H-4", H-6"), 8.05 (d, 1H, J = 2.5 Hz, H-3"), 7.95-7.81 (m, 7H, bpy (H-6a, H-5a), 7.71-7.66 (m, 2H, H-5, H-6"), 7.48 (ddd, 1H, J = 4.8 Hz, J = 1.0 Hz, H-5"), 5.40 (s, 2H, CH₂, CH₂Cl₂), 4.52-4.44 (m, 8H, CH₂, ethyl-ester), 1.46-1.41 (m, 12H, CH₃, ethyl-ester).

General Methods

NMR spectra were recorded on a Bruker Advance 600 and 400 spectrometer and referenced to the solvent signal. Elemental analysis was carried out on an Exador Analytical CE440 by Microanalytical Department of the University College Dublin. UV/Vis absorption spectra recorded on Varian Cary 50 spectrophotometer at 20 ± 1°C in a 1 cm pathlength quartz cuvette. Acetonitrile for spectrophotometric measurements was purchased from Aldrich in spectrograde and used as received.

Photophysical characterisation

Emission and excitation spectra were obtained on a Perkin Elmer LS 50B at 20 ± 1°C. The emission quantum yields were measured in de-aerated acetonitrile solution by absorbance matching at wavelength of excitation respectively to the [Ru(bpy)₃]²⁺ standard with quantum yield, Φ = 0.04. Excited-state lifetimes were measured by time-correlated single photon counting on an Edinburgh Analytical Instruments TCSPC instrument (at 293 K) in deaerated acetonitrile solution. Samples were excited with a LED at 360 nm.

DFT calculations

All calculations were carried out with the Gaussian 09 program suite.¹⁹ The compounds, **2a**, and **2b** were optimized using the M06 functional. The MWB28²⁰ basis with an effective core potential used for the heavy Ru and Pd atoms while 6-31G(d) was used for the remainder. Tight convergence criteria were applied for the geometry optimization process and local minima were confirmed by frequency calculation. All calculations were carried out in the presence of a solvent sphere, which was modelled by the IEF-PCM²¹ method in acetonitrile (ε = 35.688000). Orbital contributions were calculated by a Mulliken population analysis and evaluated using GaussSum.²²

Photocatalysis

All manipulations were carried out under strictly anaerobic inert conditions. Acetonitrile was dried over calcium hydride and triethylamine over sodium according to common procedures and freshly distilled under nitrogen prior to use. Photocatalytic hydrogen production experiments were carried out using a

home-built air-cooled apparatus (at 22 °C) under constant irradiation (LED 470 nm) of the sample. For the photocatalysis experiments 2 cm³ of the sample solution were added to GC vials (total volume 5 cm³, diameter 13 mm, 3 cm³ headspace) in the dark and under a stream of nitrogen. The vials were closed with gas-tight septum caps. A typical sample solution was prepared by mixing 0.65 cm³ of a 1.8 × 10⁻⁴ M Ru/Pd complex in acetonitrile, 0.6 ml of triethylamine, 0.0 – 0.2 ml (0 – 10 vol%) of water and 0.55 – 0.75 ml of anhydrous acetonitrile. Subsequently, the GC vials were irradiated at 470 nm using an LED for 18 h. After irradiation, 20 µl samples were drawn from the headspace with a gas tight syringe (50 µl, SGE Analytical Science) and determined by GC, a Varian CP3800 chromatograph, with a thermal conductivity detector and a CP7536 Plot Fused Silica 25 MX (MMID column (length 25 m, layer thickness 30 µm) with nitrogen carrier gas (purity 99.999 %). GC was calibrated using 100% hydrogen gas. The obtained signal (retention time for H₂ = 1.58 min) was plotted against the calibration curve and multiplied accordingly to determine the total amount of hydrogen in the headspace. The LED-torch consists of a stick-shaped printed board (19 × 1 cm) with 30 LEDs (Kingbright, type L-7113PBC-G, 470 ± 20 nm) with a luminous efficiency of 2000 mcd. LEDs are soldered closely on front and backside in a range of 9 cm. The torch was placed within the home built reactor.

Acknowledgments

This research is supported by the EPA grant 2008-ET-MS-3-S2 and SFI Grants No. 07/SRC/B108/RFP/CHE1349, SFI/TIDA/E2763, SFI/TIDA/2435.

Keywords: Photocatalytic hydrogen generation, *inter*-molecular photocatalysis, *intra*-molecular photocatalysis, supramolecular assemblies, heterodinuclear photocatalyst

References

- [1] a) E. Fujita, *Coord. Chem. Rev.*, **1999**, *185*, 373; b) A. J. Morris, G. J. Meyer and E. Fujita, *Chem. Res.* **2009**, *42*, 1983; c) T. S. Teets and D. G. Nocera, *Chem. Commun.* **2011**, *47*, 92; d) S. Rau, D. Walther, J.G. Vos, *Dalton Trans.* **2007**, 915; e) S. Losse, J. G. Vos and S. Rau, *Coord. Chem. Rev.* **2010**, *254*, 2492; f) V. Artero, M. Chavarot-Kerlidou, M. Fontecave, *Angew. Chem., Int. Ed.* **2011**, *50*, 7238; g) H. Ozawa and K. Sakai, *Chem. Commun.* **2011**, *47*, 2227; h) A. Inagaki, M. Akita, *Coord. Chem. Rev.* **2010**, *254*, 1220; i) H. Takeda, O. Ishitani, *Coord. Chem. Rev.* **2010**, *254*, 346; j) W. T. Eckenhoff, R. Eisenberg, *Dalton Trans.* **2012**, *41*, 13004; k) P. D. Frischmann, K. Mahata, F. Wurthner, *Chem. Soc. Rev.* **2013**, *42*, 1847; l) Y. Halpin, M.T. Pryce, S. Rau, D. Dini, J.G Vos *Dalton Trans.* **2013**, *42*, 16243.
- [2] a) M. Schulz, M. Karnahl, M. Schwalbe, J. G. Vos, *Coord. Chem. Rev.* **2012**, *256*, 1682; b) G. Singh. Bindra, M. Schulz, A. Paul, R. Groarke, S. Soman, J. L. Inglis, W., R. Browne, M. Pfeffer, S. Rau, B. J. MacLean, M. T. Pryce, J. G. Vos *Dalton Trans.* **2012**, *41*, 13050.

- [3] a) G. Singh Bindra, M. Schulz, A. Paul, S. Soman, R. Groarke, J. Inglis, M.T. Pryce, W. R. Browne, S. Rau, B. J. Maclean, J. G. Vos *Dalton Trans.* **2011**, 40, 10812; b) T. Kowacs, Q. Pan, P. Lang, L. O'Reilly, S. Rau, W. R. Browne, M. T. Pryce, A. Huijser, J. G. Vos. *Faraday Discuss.* **2015**, 185, 143.
- [4] M. G. Pfeffer, T. Kowacs, M. Wächtler, J. Guthmuller, B. Dietzek, J. G. Vos, Sven Rau, *Angew. Chem. Int. Ed. Engl.* **2015**, 54, 6627.
- [5] Y. Pellegrin, F. Odobel, *Comptes Rendus Chim.* **2016**, DOI 10.1016/j.crci.2015.11.026.
- [6] A. Paul, D. Connolly, M. Schulz, M. T. Pryce and J. G. Vos, *Inorg Chem.* **2012**, 51, 1977–1979.
- [7] a) A. Hagfeldt, M. Grätzel, *Acc. Chem. Res.* **2000**, 33, 269; b) M. Braumüller, M. Schulz, M. Staniszewska, D. Sorsche, M. Wunderlin, J. Popp, J. Guthmuller, B. Dietzek, S. Rau, *Dalton Trans.* **2016**, 45, 9216; c) M. Braumüller, M. Schulz, D. Sorsche, M. Pfeffer, M. Schaub, J. Popp, B.-W. Park, A. Hagfeldt, B. Dietzek, S. Rau, *Dalton Trans.* **2015**, 44, 5577; d) M. Bräutigam, J. Kubel, M. Schulz, J. G. Vos, B. Dietzek, *Phys. Chem. Chem. Phys.* **2015**, 17, 7823.
- [8] T. Kowacs, L. O'Reilly, Q. Pan, A. Huijser, P. Lang, S. Rau, W. R. Browne, M. T. Pryce, J. G. Vos, *Inorg. Chem.* **2016**, 55, 2685–2690.
- [9] L. Cassidy, S. Horn, L. Cleary, Y. Halpin, W. R. Browne, J. G. Vos, *Dalton Trans.* **2009**, 3923.
- [10] Y. Halpin, L. Cleary, L. Cassidy, S. Horne, D. Dini, W. R. Browne, J. G. Vos, *Dalton Trans.* **2009**, 4146.
- [11] Y-Q Fang and G.S. Hanan, *Synlett.* **2003**, 34, 852.
- [12] Q. Pan, F. Mecozzi, J. P. Korterik, D. Sharma, J. L. Herek, J. G. Vos, W. R. Browne, A. Huijser, *J Phys. Chem.* **2014**, 118, 20799.
- [13] J. M. Calvert, J. V. Caspar, R. A. Binstead, T. D. Westmoreland, T. J. Meyer, *J. Am. Chem. Soc.* **1982**, 104, 6620.
- [14] M. G. Pfeffer, B. Schäfer, G. Smolentsev, J. Uhlig, E. Nazarenko, J. Guthmuller, C. Kuhnt, M. Wächtler, B. Dietzek, V. Sundström, *Angew. Chem. Int. Ed.* **2015**, 54, 5044.
- [15] Q. Pan, L. Freitag, T. Kowacs, J. C. Falgenhauer, J. P. Korterik, D. Schlettwein, W. R. Browne, M. T. Pryce, S. Rau, L. Gonzalez, J. G. Vos, A. Huijser, *Chem Commun.* **2016**, 52, 9371.
- [16] B.P. Sullivan, D.J. Salmon and T.J. Meyer, *Inorg. Chem.* **1978**, 17, 3334.
- [17] a) T.E. Keyes, E. Müller, P. Pechy, M. Grätzel, J.G. Vos. *J. Chem. Soc., Dalton Trans.* **1999**, 2705; b) W. R. Browne, C. M. O'Connor, J. S. Killeen, A. L. Guckian, M. Burke, P. James Burke, J.G. Vos, *Inorg. Chem.* **2002**, 41, 4245.
- [18] M. Montalti, A. Credi, L. Prodi, M. T. Gandolfi, *Handbook of Photochemistry*, **2006**, CRC P (Taylor and Francis group), 10, 574.
- [19] M. J. Frisch, G. W. Trucks, H. B. Schlegel, G. E. Scuseria, M. A. Robb, J. R. Cheeseman, G. Scalmani, V. Barone, B. Mennucci, G. A. Petersson, H. Nakatsuji, M. Caricato, X. Li, H. P. Hratchian, A. F. Izmaylov, J. Bloino, G. Zheng, J. L. Sonnenberg, M. Hada, M. Ehara, K. Toyoda, R. Fukuda, J. Hasegawa, M. Ishida, T. Nakajima, Y. Honda, O. Kitao, H. Nakai, T. Vreven, J. J. A. Montgomery, J. E. Peralta, F. Ogliaro, M. Bearpark, J. J. Heyd, E. Brothers, K. N. Kudin, V. N. Staroverov, R. Kobayashi, J. Normand, K. Raghavachari, A. Rendell, J. C. Burant, S. S. Iyengar, J. Tomasi, M. Cossi, N. Rega, J. M. Millam, M. Klene, J. E. Knox, J. B. Cross, V. Bakken, C. Adamo, J. Jaramillo, R. Gomperts, R. E. Stratmann, O. Yazyev, A. J. Austin, R. Cammi, C. Pomelli, J. W. Ochterski, R. L. Martin, K. Morokuma, V. G. Zakrzewski, G. A. Voth, P. Salvador, J. J. Dannenberg, S. Dapprich, A. D. Daniels, O. Farkas, J. B. Foresman, J. V. Ortiz, J. Cioslowski, D. J. Fox, **2009**.

-
- [20] X. Cao, *J. Mol. Struct. THEOCHEM*, **2002**, 581, 139.
- [21] J. Tomasi, B. Mennucci, and R. Cammi, *Chem. Rev.*, **2005**, 105, 2999.
- [22] N. M. O'Boyle, A. L. Tenderholt, K. M. Langner, *J. Comput. Chem.*, **2008**, 29, 839.

Accepted Manuscript